

Valence quarks and k_T factorisation

Michal Deák, Hannes Jung, Krzysztof Kutak *

Deutsches Elektronen-Synchrotron
Notkestrasse 85, 22607 - Hamburg, Germany

We study in the k_T factorisation framework jet production at LHC energies. In particular we are interested in valence quark and gluon initiated jets. The calculation of the relevant hard matrix element is presented. A CCFM like evolution equation for valence quark distribution is solved and the cross section for valence quark and gluon initiated process is calculated using Monte Carlo event generator CASCADE.

1 Introduction

Collisions at LHC will hopefully answer many so far unanswered questions about Standard Model and beyond. Here we focus on details of jet production at LHC due to valence quark - gluon interaction. This process is of interest since it may shed light on so called phenomenon of saturation and it may test different factorisation schemes. This process will be measured at central and forward calorimeters (Castor in CMS).

In first step we calculate hard matrix element for $g^*q \rightarrow gq$, then we calculate the total cross section and show the differential cross sections as functions of E_T and η distribution of produced jets. To calculate jet production we use CASCADE Monte Carlo event generator [1].

2 Matrix element for $g^*q \rightarrow gq$

We begin our study by calculating matrix element for $g^*q \rightarrow gq$ (this has been calculated in [2] but in a different context). In our studies we assume Regge kinematics which means that we are going to work in regime where the total center of mass energy squared of proton-proton collision is much larger than any other scale involved in the collision. This practically means:

$$s \gg \hat{s}, |\hat{t}|, |\hat{u}|$$

where: $s = (p_A + p_B)^2$, $\hat{s} = (k + q)^2$, $\hat{u} = (k - q')^2$, $\hat{t} = (k - k')^2$ (see Figure 1). To calculate the amplitude we have to sum expressions for diagrams in Figure 1. We proceed by using Sudakov decomposition of four momenta:

$$\begin{aligned} k &= x_g p_A + z_g p_B + k_T \\ q &= x_q \\ k' &= x_{g'} p_A + z_{g'} p_B + k'_T \\ q' &= z_{q'} p_A + x_{q'} p_B + q'_T \end{aligned}$$

Where x_q is longitudinal momentum fraction of incoming quark, x_g is a longitudinal momentum fraction of incoming gluon ($x_g \sim 10^{-5}$), k_T is its transverse momentum. $x_{q'}$ is a longitudinal momentum fraction of outgoing quark, q'_T is its transverse momentum. $x_{g'}$

*Presented by Krzysztof Kutak at the XVI Workshop on Deep Inelastic Scattering (DIS2008), London, 7 - 11 April 2008.

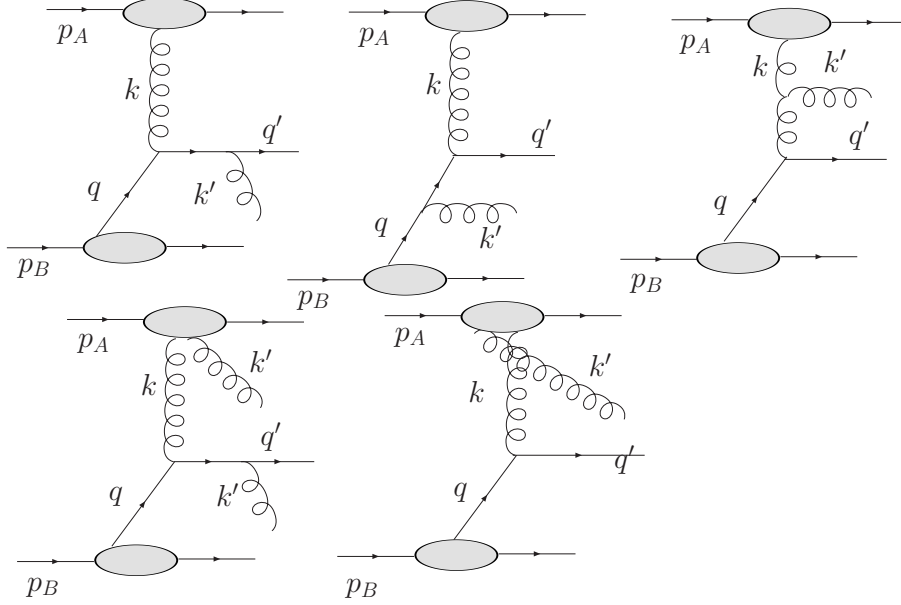


Figure 1: Diagrams which contribute to QCD Compton scattering in Feynman gauge. In calculation we put for proton A an auxiliary quark impact factor and gluon with momentum flow k is of shell. Proton B is factored out and the quark with momentum q is considered to be on-shell

is a longitudinal momentum fraction of outgoing gluon, k'_T is its transverse momentum. In calculations of matrix element the interesting kinematical regime is where the incoming gluon carries low longitudinal momentum fraction ($x_g \sim 10^{-5}$) and we can make the eikonal approximation to the current. On the other hand since the incoming quark carries high momentum fraction ($x_q \sim 10^{-1}$) we take the exact expression for the current. The resulting formula for the matrix element squared for $g^*q \rightarrow gq$ for unpolarized quarks and gluons, after summing and averaging over colors of final and initial state particles, reads:

$$|\mathcal{M}|^2 = (4\pi)^2 \alpha_S^2 \frac{x_g^2 s^2 (x_q^2 + x_q'^2)}{18 \hat{s} \hat{u} \hat{t}} \left(\frac{\hat{s}(8x_q + x_q') - \hat{u}(8x_q' + x_q)}{(x_q - x_q')} - \mathbf{k}^2 \right)$$

From the expression for the matrix element squared we can see that in addition to term formally equal to the collinear result we get a term proportional to \mathbf{k}^2 . This matrix element has interesting structure of singularities. Singularities appear in 4 different points in the phase space when one of the final state partons four-momentum is collinear with a four-momentum of a quark in the initial state (taking also the quark with the momentum p_A into account).

3 Numerical results

The cross section in k_T factorisation approach can be schematically written as:

$$d\sigma(pp \rightarrow gqX) \sim \mathcal{A}(x_g, \vec{k}_\perp^2, \mu^2) \otimes M(g^*q \rightarrow gqX) \otimes \mathcal{Q}(x_q, \vec{q}_\perp^2, \mu^2)$$

where \otimes stands for integration over longitudinal, angular and transversal degrees of freedom, μ_1, μ_2 are the factorisation scales. In the formula above $\mathcal{A}(x_g, \vec{k}_\perp^2, \mu_1^2)$ is the unintegrated, gluon density obtained by solving the CCFM evolution equation and $\mathcal{Q}(x_q, \vec{q}_\perp^2, \mu_2^2)$ is the

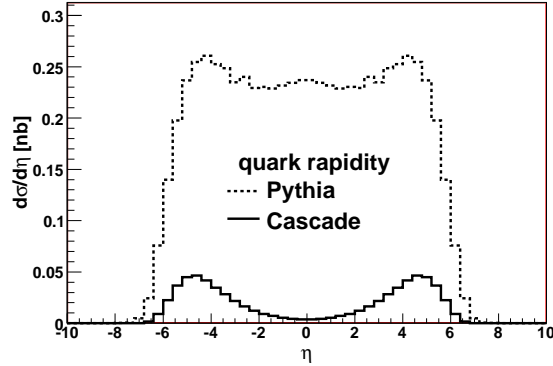


Figure 2: Final quark pseudorapidity distribution .

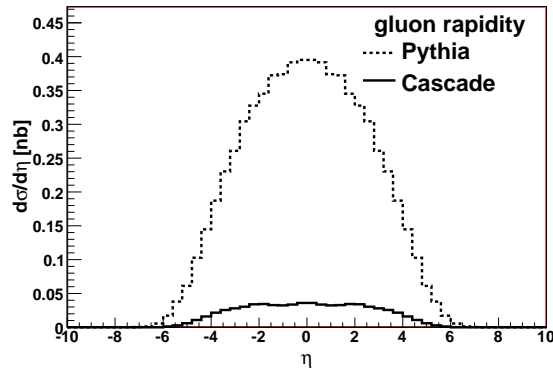


Figure 3: Final gluon pseudorapidity distribution .

unintegrated valence quark density obtained from CCFM-like equation which is needed for technical reasons in Monte Carlo simulation. The initial valence quark distribution is provided by CTEQ 6.1 set. In our calculations we use running coupling constant and we make a 10GeV cut on transverse momenta of out going jets. This cut is motivated by the experimental setup where jets at lower momenta are hardly measurable. This cut removes the collinear configuration singularities of the matrix element. As a first observable we calculated total cross section for two jet production in considered kinematical region and we obtained 0.17mb . As other observable we investigate the rapidity distributions of the produced jets. The results of the calculation of the rapidity distributions of outgoing partons is presented in Figure 2. As expected, the quark initiated jet is in the forward rapidity region while the gluon initiated jet is in the central rapidity region. We make here a comparison to PYTHIA Monte Carlo prediction. The difference between distributions is due to missing sea quark contribution in CASCADE. The other interesting observable is the transverse energy E_T (Figure 4) and η distributions (Figure 5) of produced jets. The

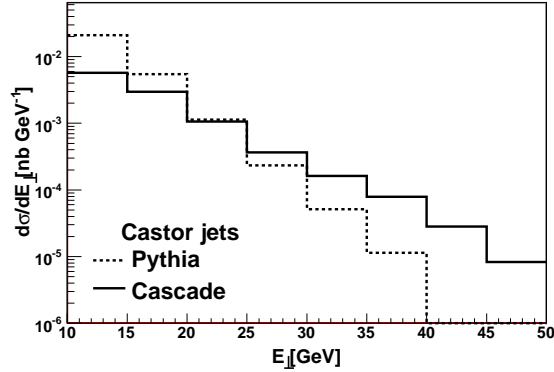


Figure 4: Transverse energy distribution of produced jet in Castor calorimeter range.

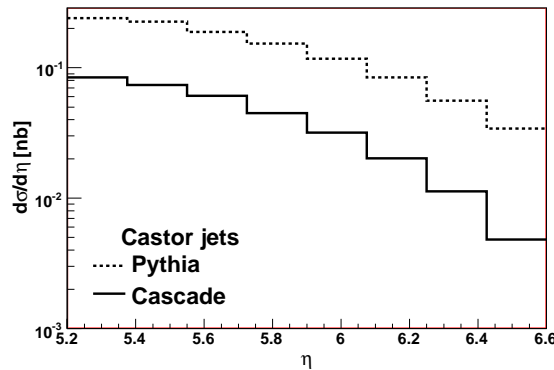


Figure 5: Pseudorapidity distribution of produced jet in Castor calorimeter range.

first of this distributions is of particular importance because it shows visible difference due to different assumptions about underlying physics. For example one sees that CASCADE including the off shell matrix element favors a harder spectrum than PYTHIA which is based on collinear factorisation. The η distributions generated by CASCADE and PYTHIA differ because missing sea quarks in our approach. However, this difference is small in region of our interest (large E_T).

4 Bibliography

References

- [1] H. Jung, Comput.Phys.Commun. 143 (2002) 100-111
- [2] M. Ciafaloni, Phys. Lett. **B429** 363 (1998);
- [3] Slides:
<http://indico.cern.ch/contributionDisplay.py?contribId=42&sessionId=8&confId=24657>